Classification of myocardial infarction with multi-lead ECG signals and deep CNN ☆

Ulas Baran Baloglu [a], Muhammed Talo [a], Ozal Yildirim [a,*], Ru San Tan [b,c], U Rajendra Acharya [d,e,f]

[a] *Department of Computer Engineering, Munzur University, Tunceli 62000, Turkey*
[b] *Department of Cardiology, National Heart Centre Singapore, Singapore*
[c] *Duke-NUS Medical School, Singapore*
[d] *Department of Electronics and Computer Engineering, Ngee Ann Polytechnic, Singapore*
[e] *Department of Biomedical Engineering, School of Science and Technology, Singapore School of Social Sciences, Singapore*
[f] *School of Medicine, Faculty of Health and Medical Sciences, Taylor's University, Subang Jaya 47500, Malaysia*

A R T I C L E   I N F O

A B S T R A C T

Myocardial infarction (MI), commonly known as heart attack, causes irreversible damage to heart muscles and even leads to death. Rapid and accurate diagnosis of MI is critical to avoid death. Blood tests and electrocardiogram (ECG) signals are used to diagnose acute MI. However, for an increase in blood enzyme values, a certain time must pass after the attack. This time lag may delay MI diagnosis. Hence, ECG diagnosis is still very important. Manual ECG interpretation requires expertise and is prone to inter-observer variability. Therefore, computer aided diagnosis may be useful in automatic detection of MI on ECG. In this study, a deep learning model with an end-to-end structure on the standard 12-lead ECG signal for the diagnosis of MI is proposed. For this purpose, the most commonly used technique, convolutional neural network (CNN) is used. Our trained CNN model with the proposed architecture yielded impressive accuracy and sensitivity performance over 99.00% for MI diagnosis on all ECG lead signals. Thus, the proposed model has the potential to provide high performance on MI detection which can be used in wearable technologies and intensive care units.

© 2019 Elsevier B.V. All rights reserved.

1. Introduction

Myocardial infarction (MI) is heart muscle damage that results from interruption of tissue blood flow caused by occlusion of coronary arteries due to thrombus. It potentially causes permanent damage (myocardial tissue death) unless there is prompt intervention to open up the coronary artery either by percutaneous or surgical methods. Hence, early identification and diagnosis are crucial to avert MI complications like heart failure, arrhythmia and death. Diagnosis of acute MI is typically made using electrocardiography (ECG), which requires expert knowledge and is prone to inter-observer variability. With rapid technological advances in ECG recording devices, related processing equipment and analytics, 12-lead ECG data can be optimized for diagnosis of MI and other heart diseases, especially with the use of computer-aided methods [1–3].

The ECG provides information about both the presence and localization of MI. MI characteristics include ST-segment elevation,

abnormal Q wave appearance, and T-wave inversion [4]. These are commonly used for classification of feature vectors [5–7]. Acharya et al. [8] suggested an approach for automated MI detection and localization on 12-lead ECG where they decomposed the ECG signals to four levels with wavelet transform and classified 12 nonlinear features on the signals with k-nearest neighbor (KNN). From previous studies, KNN classifier has been successfully applied for the detection of MI [5]. For MI diagnosis, Kumar et al. [9] processed segmented ECG signals to decompose them into sub-band signals for extraction of sample entropy values that were later used as input for different classifiers. For decomposition of ECG signals, it is also feasible to use stationary wavelet transform [10] as it is known that discrete wavelet transform performs well with ECG signals [11]. Principal Component Analysis (PCA) and polynomial approximation have been combined in the feature extraction phase of MI classification to improve the classification performance [12]. Optimization algorithms can be used to improve the performance of the feature extraction phase [13,35]. Several studies target the classification part of these automated diagnosis models. Dohare et al. [14] used Support Vector Machine (SVM) classifier to develop a model that did not need signal

---

☆ **Conflict of interest**: The authors declare no conflict of interest.
* Corresponding author.
E-mail address: oyildirim@munzur.edu.tr (O. Yildirim).

preprocessing with digital filters, band-pass filter, filter-banks, and wavelet transform. Separately, He et al. [15] developed an unsupervised classification scheme using wavelet tensor decomposition and two- dimensional Gaussian spectral clustering.

Using signal analytics, MI ECG signal appearance can be differentiated from those of other common diseases - such as bundle branch block and heart muscle defect – as well as healthy controls (HC) [4]. Acharya et al. [3] proposed a new model based on preformation of contourlet and shearlet transforms on each scalogram to derive entropies and statistical features. They used decision tree (DT) and KNN classifiers at the classification stage to obtain a single diagnostic method which can identify different cardiac abnormalities such as coronary artery disease, congestive heart failure and MI at early stages. In another study, Fujita et al. [1] proposed an automated classification that can detect cardiac abnormalities as four different classes instead of just classifying them in two classes as normal and abnormal. Tripathy et al. [16] used principal component multivariate multi-scale sample entropy as a measure for classifying different cardiovascular diseases such as cardiomyopathy, MI and hypertrophy. These studies pave the way for the development of an effective tool that can detect different cardiac abnormalities simultaneously from the same 12-lead ECG data. Logically, smart wearable can host these solutions if they can be implemented in a way that reduced energy consumption [17]. Sadhukhan et al. [18] used harmonic phase distribution pattern of ECG data to implement a portable healthcare device prototype for identification of different cardiac abnormalities. Padhy and Dandapat [19] reduced the dimension of features by applying third-order tensors, effectively accelerating computation times.

In previous studies [1,3–23,35–37], linear or nonlinear ECG signal feature sets have been usually generated using various feature extraction methods. These feature sets are sometimes reduced using feature selection algorithms to lower-size feature vectors. The features, typically handcrafted, are input to a shallow classifier for signal classification. Although still widely used in the field of machine learning, these approaches are gradually supplanted by deep learning algorithms that can gather all these processes in a single structure as demonstrated in [24–30]. Lodhi et al. [24] employed one Convolutional Neural Network (CNN) for each lead of the 12-lead ECG data so that 12 CNNs constituted a voting mechanism for MI detection. Using such a high number of CNNs would not be feasible for portable health care devices. Lui and Chow [25] developed a classifier that combined both convolutional and recurrent neural networks, achieving a better performance than CNN alone. Acharya et al. [26] employed the CNN model on 12-lead ECG

for accurate automated detection of MI even with noise in ECG data.

The primary motivation of this study is to develop an efficient automated model for diagnosis of MI on ECG that can feasibly be implemented on portable healthcare devices. In the machine learning techniques, we manually extract the features from the raw ECG data with hand-crafted techniques or use the features learned by other machine learning models. Then the extracted features are classified by a classifier. We have used deep learning methods which automatically extract the hidden signatures from the raw data and use this knowledge for the classification. For this purpose, a new efficient CNN model is proposed. This end-to-end model successfully classifies 12-lead ECG signals without requiring a handcrafted feature extraction stage. The main difference of the proposed model from previous studies lies in its high accuracy and sensitivity performance on all ECG lead signals.

2. Material and methods

In this study, a CNN-based approach that works with end-to-end architecture has been proposed for the automatic detection of MI on standard 12-lead ECG data. A CNN model is proposed as it provides high recognition on all lead signals. This model is individually trained and tested for each lead signal. Thus, instead of developing a different model for each of these signals, a flexible deep learning model was developed that could recognize MI types for all lead signals. A block representation of the method used in this study is given in Fig. 1.

2.1. Dataset

In this study the open-access Physiobank (PTB) ECG database is used [31]. The data comprise ECG records of 52 normal subjects and 148 MI patients. On 12-lead ECG, ten typical geographical MI locations can be described based on presence of MI ECG perturbations in various groupings of contiguous ECG vectors: anterior (A), anterior lateral (AL), anterior septal (AS), inferior (I), inferior lateral (IL), inferior posterior (IP), inferior posterior lateral (IPL), lateral (L), posterior (P) and posterior lateral (PL). ECG signal from each lead is digitized at sampling rate of 1000 Hz. Pre-processing based on wavelet transform is applied to remove noise and baseline wander. The pre-processed signals are then segmented to detect the ECG R-peak (the tallest positive point of the QRS complex in each ECG cycle). To ensure adequate coverage of the QRS complex and following ST segment – both of which are altered in MI - a total of
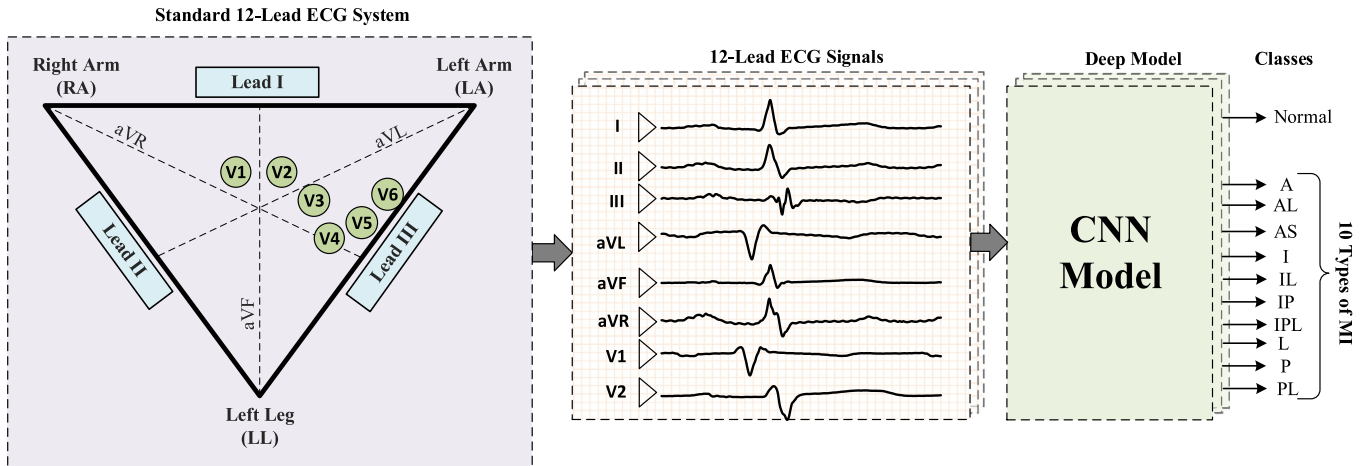

Fig. 1. The block representation of the method used in the study.

Table 1
12 lead beat numbers contained in the ECG dataset.

Classes	Number of beats												Total (Percentage)
	Leads												
	I	II	III	aVR	aVL	aVF	V$_1$	V$_2$	V$_3$	V$_4$	V$_5$	V$_6$	
A	4902	4861	4993	4720	4882	4941	4742	4741	4743	4745	4743	4741	57,754 (9.44%)
AL	6424	6467	6360	6579	6676	6520	6501	6538	6540	6397	6589	6514	78,105 (12.77%)
AS	8146	8024	8260	8153	8146	8567	8152	8148	8238	8429	8151	8152	98,566 (16.12%)
H	10,598	10,546	10,574	10,494	10,537	10,472	10,482	10,483	10,450	10,371	10,322	10,323	125,652 (20.55%)
I	10,592	10,691	11,522	10,588	11,161	11,008	10,502	10,671	10,711	10,591	10,589	10,589	129,215 (21.13%)
IL	5911	5888	5919	5911	5909	6047	5900	5932	5914	5912	5861	5882	70,986 (11.61%)
IP	48	48	48	48	48	48	48	48	48	48	48	48	576 (0.09%)
IPL	2516	2512	2517	2516	2518	2520	2515	2503	2516	2516	2516	2516	30,181 (4.93%)
L	459	459	460	459	470	459	459	459	459	459	459	459	5520 (0.9%)
P	460	460	459	460	460	460	460	461	463	460	460	460	5523 (0.9%)
PL	777	772	777	778	779	778	779	778	777	777	777	777	9326 (1.52%)
Total	*50,833*	*50,728*	*51,889*	*50,706*	*51,586*	*51,820*	*50,540*	*50,762*	*50,859*	*50,705*	*50,515*	*50,461*	**611,404 (100%)**
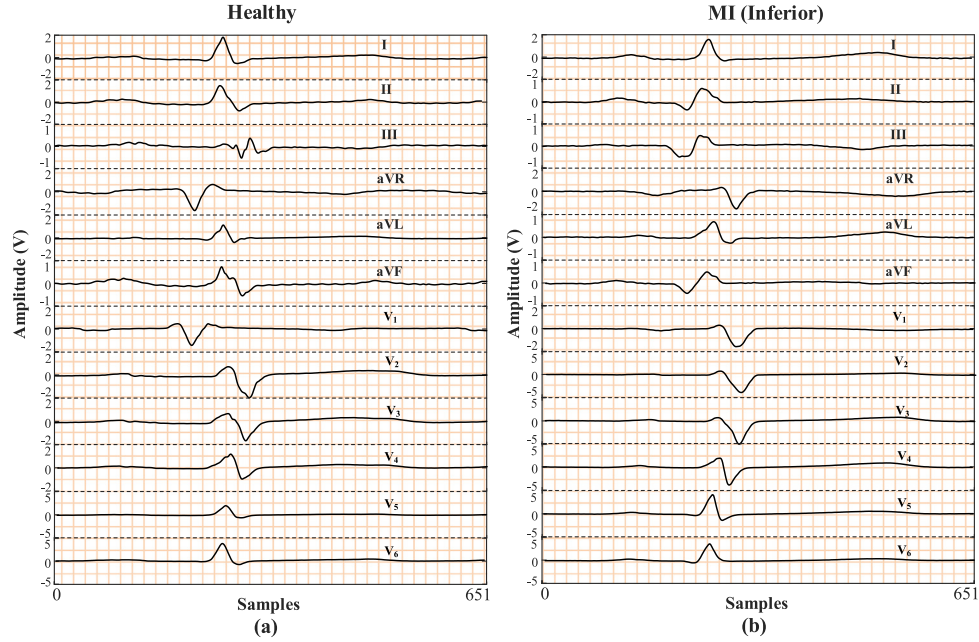
Fig. 2. 12 lead ECG signal samples for a) Healthy and b) Inferior MI subjects.

651 sample pulses are obtained, with 250 and 400 samples to the left and right, respectively, of the R-peak. Table 1 shows the distribution of numerical data for healthy (H) and MI beats for the 12-lead ECG.

20.55% (125652 beats) of the total of 611,404 beats belongs to healthy subjects. Among MI subjects, the highest and lowest number of beats are in I (129215 beats, 21.13%) and IP classes (576 beats), respectively. Fig. 2 shows 12-lead ECG signal segments from H and I classes.

Since each lead represents vector information from sensors placed in different geographical positions of the chest, ECG signals from each lead show different characteristics. Lead II signal is commonly used in the classification of ECG signals [9,10,28,30]. Examples of lead II signal waveform readouts of healthy and various MI localizations in the study dataset are depicted in Fig. 3.

2.2. The proposed deep CNN model

In this study, a deep learning model is created to provide high recognition performance on ECG signals from all leads based on CNN, which has been optimized to include uncomplicated and standard CNN layers. The 10-layer deep CNN model with a block representation is summarized in Fig. 4. Healthy and MI ECG beats, each with 651 samples, feed into the input layer of this model. They go through hierarchically ordered convolution and maxpooling layers and transform into feature maps of different sizes. In the dense layer, an automatic prediction of the classes is provided by learning of these feature maps. We have used dropout technique to avoid overfitting during training of the model. By using dropout technique, we randomly turned off 20% of neurons during training. Additionally, we did not train the model for large number of epochs. In each epoch, the model examines the whole training dataset. If the epoch number is chosen to be too big, a model can memorize the training data. In order for readers to be able to reproduce the model proposed in this study, Table 2 details the specific of each layer's parameters.

3. Experimental results

Experimental studies for all leads in the dataset are conducted separately using the same deep model. Without changing any parameters of the model, only the dataset is changed and applications are implemented. In the evaluation of the model, the data for ECG signals from all leads are partitioned for 70% training, 15% validation and 15% testing respectively. The model, which is trained with training and validation data, is then tried on the

Table 2
Details of each layer's parameters of the proposed deep CNN model.

| No	Layer name	Layer parameters	Output shape	Number of Params
1	Conv 1D	64×5, *Strides*=1, *Input shape*=(651, 1), *Activation*=ReLU	647×64	384
2	Conv 1D	128×3, *Strides*=1, *Activation*=ReLU	645×128	24,704
3	MaxPooling1D	*Pool size*=2, *Strides*=2	322×128	0
4	Dropout	*Rate*=0.2	322×128	0
5	Conv 1D	128×13, *Strides*=1, *Activation*=ReLU	310×128	213,120
6	Conv 1D	256×7, *Strides*=1, *Activation*=ReLU	304×128	229,632
7	MaxPooling1D	*Pool size*=2, *Strides*=2	152×256	0
8	Flatten	–	38,912	0
9	Dense	64, *Activation*=ReLU, *Dropout rate*=0.2	64	2,490,432
10	SoftMax	11, *Activation*=SoftMax	11	715
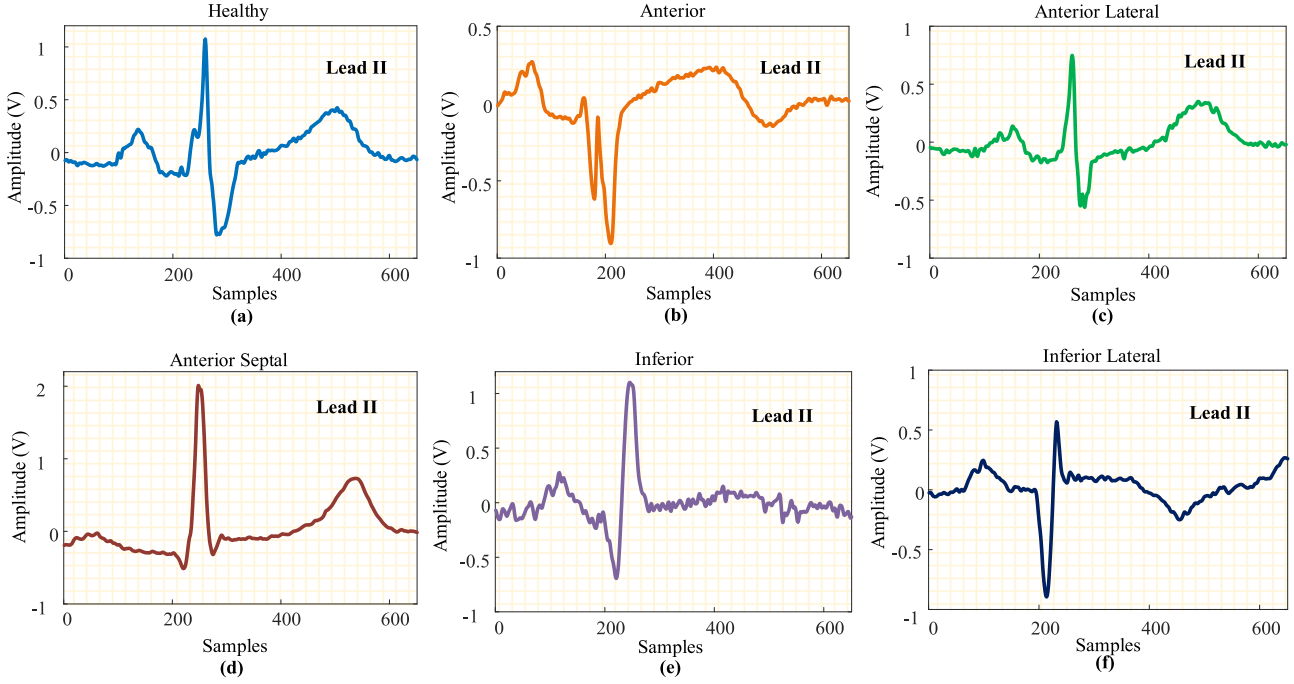
Fig. 3. Lead II waveforms of some ECG signals in the data set: a) healthy, b) anterior, c) anterior lateral, d) anterior septal, e) inferior, f) inferior lateral.
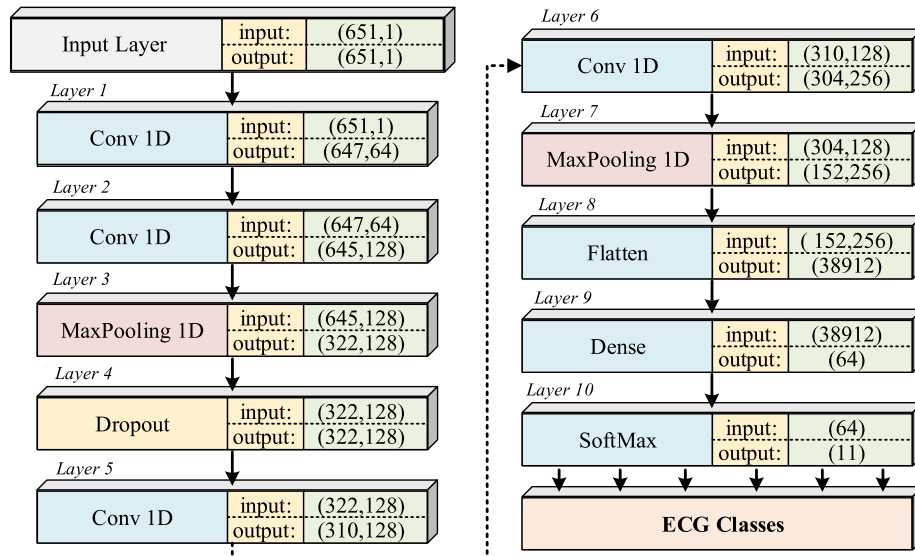

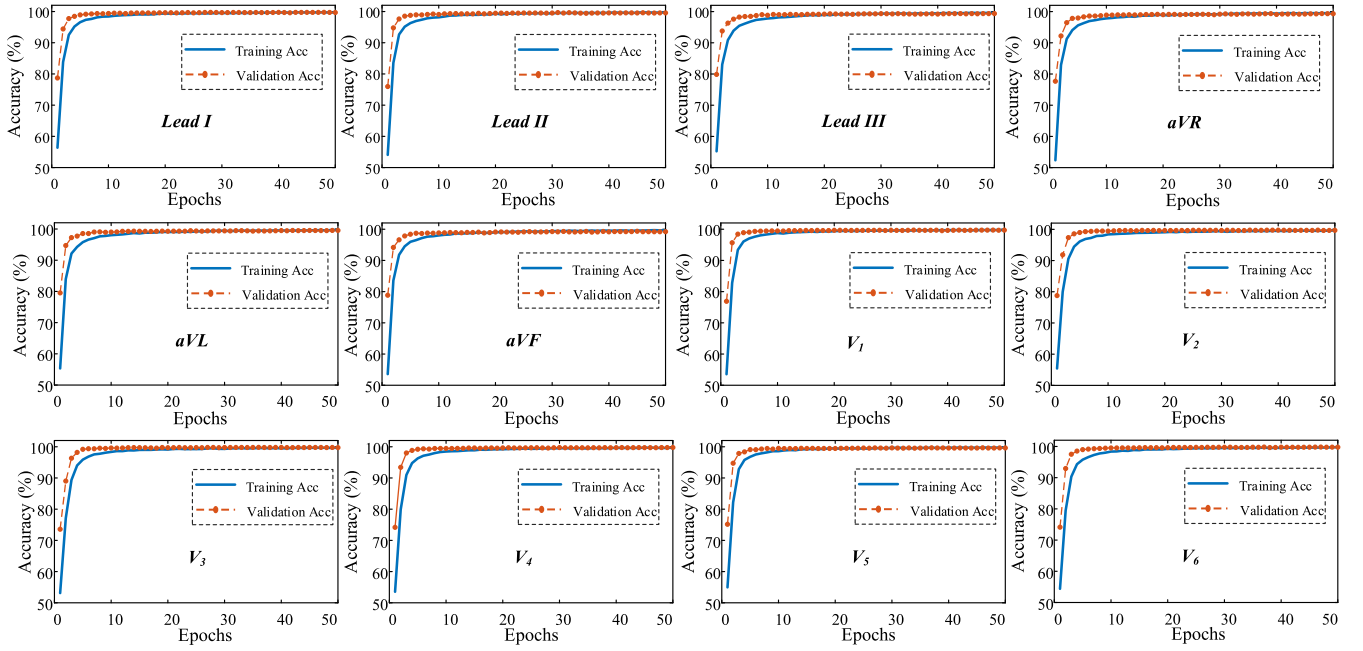**Fig. 4.** Block representation of the proposed deep CNN model.

Fig. 5. Performance graphs for ECG signal from each lead of the CNN model at the training stage.

unseen test data. All experiments are conducted on a Linux Server (Ubuntu 16.04.4) with NVIDIA GeForce GTX 1080 Ti (11 GB). Keras deep learning library is used for deep learning algorithms [32]. For the hyperparameters of the proposed model, learning rate is set to 10–3 and decay 10–4. Additionally, 64 batch size and 50 epochs are used for each training phase. Adam optimizer and categorical cross entropy loss function are selected. When the CNN model is individually trained for all the ECG lead signals during the 50-epoch period, the training accuracy and validation accuracy results are presented in Fig. 5.

In the training phase, it is seen that the proposed CNN model performance exceeds 99% in all lead. The model successfully completed the learning process of ECG signals at the end of a short period of time (10 epochs). No overfitting problem occurred in the model during the training phase. After the training, the proposed CNN model is applied to the test data. Table 3 shows the performance of the trained CNN model at the end of 50th epoch on test data from all ECG leads.

The CNN model recognized the test data for all leads with a high accuracy rate of over 99%. The highest classification performance is 99.78% for lead V4 and 99.75% for lead V5. These excellent results indicate that the proposed model is effective for all

Table 3
The accuracy of the trained CNN model on the test data.

ECG signals	Training accuracy	Validation accuracy	Testing accuracy
Lead 1 (I)	99.71%	99.68%	99.61%
Lead 2 (II)	99.70%	99.56%	99.53%
Lead 3 (III)	99.55%	99.35%	99.36%
Lead 4 (aVR)	99.47%	99.31%	99.57%
Lead 5 (aVL)	99.64%	99.54%	99.50%
Lead 6 (aVF)	99.66%	99.21%	99.37%
Lead 7 (V$_1$)	99.72%	99.70%	99.63%
Lead 8 (V$_2$)	99.64%	99.69%	99.78%
Lead 9 (V$_3$)	99.68%	99.73%	99.67%
Lead 10 (V$_4$)	99.67%	99.76%	99.78%
Lead 11 (V$_5$)	99.73%	99.63%	99.75%
Lead 12 (V$_6$)	99.72%	99.77%	99.72%
Average:	*99.65%*	*99.57%*	*99.60%*

lead signals. Fig. 6 shows the confusion matrix obtained after the trained CNN model is applied to the lead V4 test data.

The CNN model correctly recognizes the data in the IP, IPL, L, P and PL MI classes as shown in the confusion matrix when the lead V4 ECG is applied to the test signals. In the healthy class containing 1562 data, 99.9% accuracy value is obtained, with only one data labelled incorrectly. The average training procedure took about 400 s for each lead and the test time took an average of 0.13 milliseconds for each ECG signal test sample. For the detailed evaluation of the model on the test data, some commonly used performance criteria are used. These criteria are precision (PRE), sensitivity (SEN), specificity (SPE) and F1-score, which are related to true positive (TP), true negative (TN), false positive (FP) and false negative rates (FN) [33,34]:

$$Accuracy(ACC) = \frac{(TP + TN)}{(TP + FP + TN + FN)} \quad (1)$$

$$Precision(PRE) = \frac{TP}{(TP + FP)} \quad (2)$$

$$Sensitivity(SEN) = \frac{TP}{(TP + FN)} \quad (3)$$

$$Specificity(SPE) = \frac{TN}{(TN + FP)} \quad (4)$$

$$F1 - Score(F1) = \frac{2 \times (SEN \times PRE)}{(SEN + PRE)} \quad (5)$$

Table 4 shows the performance values for the lead V4 ECG signal as a result of the classification of the test data.

All performance values for this lead signal are over 99%. Notably, the performances for IP, IPL, L and P MI classes are 100%. It is seen that lateral (L) and posterior (P) MI status is dominant in the groups in which CNN model has achieved full success. On the other hand, the amount of data in these classes is lower than in other classes.

As the purpose of computer aided diagnosis is to ensure efficient screening of MI and prevent missing out cases, the performance criterion SEN, which indicates that a diagnostic test actually identifies patients with the disease, is especially relevant. Accordingly, SEN values obtained from test data of all leads are

Accuracy: 99.78%

Output Class \ Target Class	A	AL	AS	H	I	IL	IP	IPL	L	P	PL
A	99.6% 735	0.1% 1	0.0% 0	0.0% 0	0.0% 0	0.0% 0	0.0% 0	0.0% 0	0.0% 0	0.0% 0	0.0% 0
AL	0.0% 0	99.4% 952	0.2% 2	0.0% 0	0.1% 1	0.2% 2	0.0% 0	0.0% 0	0.0% 0	0.0% 0	0.0% 0
AS	0.4% 3	0.2% 2	99.8% 1262	0.1% 1	0.0% 0	0.0% 0	0.0% 0	0.0% 0	0.0% 0	0.0% 0	0.0% 0
H	0.0% 0	0.0% 0	0.0% 0	99.9% 1561	0.0% 0	0.1% 1	0.0% 0	0.0% 0	0.0% 0	0.0% 0	0.0% 0
I	0.0% 0	0.1% 1	0.0% 0	0.0% 0	99.9% 1608	0.0% 0	0.0% 0	0.0% 0	0.0% 0	0.0% 0	0.0% 0
IL	0.0% 0	0.1% 1	0.1% 1	0.0% 0	0.0% 0	99.6% 854	0.0% 0	0.0% 0	0.0% 0	0.0% 0	0.0% 0
IP	0.0% 0	0.0% 0	0.0% 0	0.0% 0	0.0% 0	0.0% 0	100.0% 6	0.0% 0	0.0% 0	0.0% 0	0.0% 0
IPL	0.0% 0	0.0% 0	0.0% 0	0.0% 0	0.0% 0	0.0% 0	0.0% 0	100.0% 383	0.0% 0	0.0% 0	0.0% 0
L	0.0% 0	0.0% 0	0.0% 0	0.0% 0	0.0% 0	0.0% 0	0.0% 0	0.0% 0	100.0% 64	0.0% 0	0.0% 0
P	0.0% 0	0.0% 0	0.0% 0	0.0% 0	0.0% 0	0.0% 0	0.0% 0	0.0% 0	0.0% 0	100.0% 54	0.0% 0
PL	0.0% 0	0.1% 1	0.0% 0	0.0% 0	0.0% 0	0.0% 0	0.0% 0	0.0% 0	0.0% 0	0.0% 0	100.0% 110

Fig. 6. Confusion matrix obtained with test data for lead V4.

Table 4
Evaluation values of the CNN model on Lead (V4) test data.

Classes	ACC (%)	PRE (%)	SEN (%)	SPE (%)	F1 (%)	Number of Data
Anterior (A)	99.94	99.59	99.86	99.95	99.72	736
Anterior Lateral (AL)	99.85	99.37	99.47	99.90	99.42	957
Anterior Septal (AS)	99.88	99.76	99.52	99.95	99.64	1268
Healthy (H)	99.97	99.93	99.93	99.98	99.93	1562
Inferior (I)	99.97	99.93	99.93	99.98	99.93	1609
Inferior Lateral (IL)	99.93	99.64	99.76	99.95	99.70	856
Inferior Posterior (IP)	100	100	100	100	100	6
Inferior Posterior Lateral (IPL)	100	100	100	100	100	383
Lateral (L)	100	100	100	100	100	64
Posterior (P)	100	100	100	100	100	54
Posterior Lateral (PL)	99.98	100	99.09	100	99.54	111
Overall Accuracy (%) = 99.78						

Table 5
SEN values obtained for all lead ECG test data.

Leads	Sensitivity (%)										
	A	AL	AS	H	I	IL	IP	IPL	L	P	PL
1 (I)	99.72	99.79	99.13	99.75	99.80	99.40	**100**	99.74	98.64	**100**	99.02
2 (II)	99.18	99.27	99.74	99.74	99.75	99.11	**100**	98.90	**100**	**100**	**100**
3 (III)	98.58	99.15	99.19	99.45	99.82	99.30	**100**	99.45	98.48	**100**	**100**
4 (aVR)	99.45	99.08	99.51	99.93	99.80	99.53	**100**	98.96	**100**	**100**	98.41
5 (aVL)	99.23	99.04	99.50	99.62	99.87	99.32	**100**	99.43	**100**	**100**	99.18
6 (aVF)	99.07	98.75	99.59	99.74	99.75	99.05	**100**	98.22	98.46	**100**	**100**
7 (V$_1$)	98.92	99.49	99.67	**100**	99.67	99.76	**100**	99.21	**100**	**100**	99.05
8 (V$_2$)	99.18	99.79	99.75	99.86	99.93	99.88	**100**	99.73	**100**	**100**	99.15
9 (V$_3$)	99.44	99.12	**100**	99.93	99.56	99.76	**100**	99.47	**100**	**100**	**100**
10 (V$_4$)	99.86	99.47	99.52	99.93	99.93	99.76	**100**	**100**	**100**	**100**	99.09
11 (V$_5$)	99.59	99.69	99.67	99.73	99.93	99.54	**100**	**100**	**100**	**100**	**100**
12 (V$_6$)	99.44	99.41	99.83	99.93	99.73	100	**100**	98.97	**100**	**100**	**100**
Average	*99.30*	*99.33*	*99.59*	*99.80*	*99.79*	*99.53*	***100***	*99.34*	*99.63*	***100***	*99.49*

presented in Table 5. The lowest SEN values of all lead ECG signals (mean 99.30%) are for the Anterior MI class. On the other hand, IP and P MI classes show 100% SEN performance value on all lead signals. A visual comparison of ECG signals in this group and the waveforms of ECG signals in healthy class are given in Fig. 7.

As can be seen from Fig. 7, the IP and P signals appear relatively homogeneous. In contrast, ECG waveforms of healthy subjects are more heterogeneous. It did not affect the MI class also, as the CNN model can recognize the abnormal class with a high SEN of 99.80% for all leads. In other words, the proposed model is robust for the heterogeneity within ECG segments.

4. Discussion

There are many approaches for the automatic classification of MI ECG signals in the literature. The number of leads and MI classes used in these approaches differ, and should be noted when comparing their relative performances. Table 6 presents a comparison of the results of some published studies and the current proposed approach.

Acharya et al. [8] studied MI detection and localization, and reported at least a minimum performance of 86.93% for all leads. With KNN classifier, lead V3 achieved 98.74% performance on the ECG signal. Kumar et al. [9] obtained 99.31% accuracy by using lead
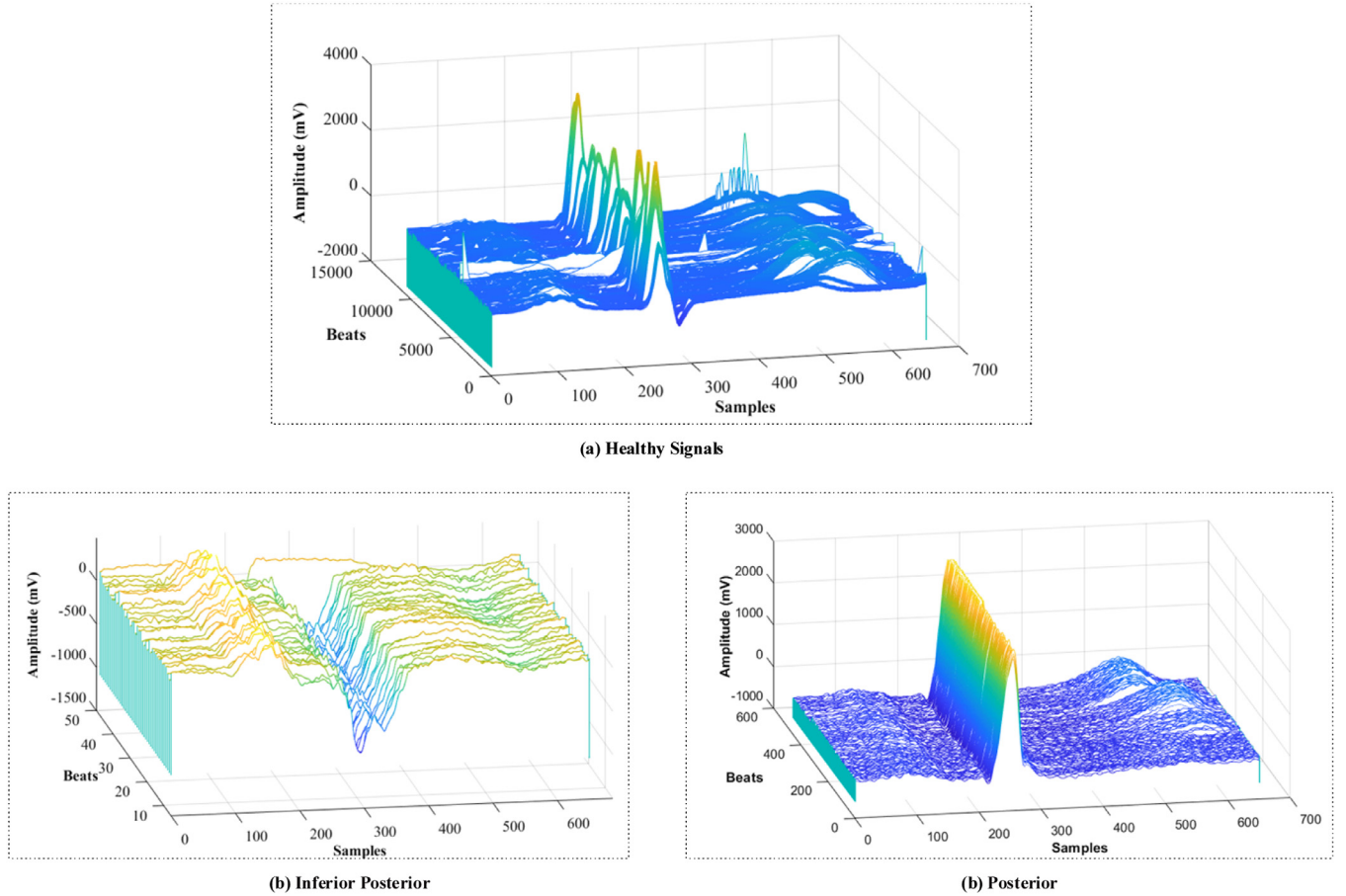
(a) Healthy Signals

(b) Inferior Posterior

(b) Posterior

Fig. 7. Healthy and some MI subject Lead 10 (V4) ECG waveforms: a) Healthy, b) Inferior Posterior, c) Posterior.

Table 6
Comparison of the methods for detection of MI on ECG.

Study	Lead/Class	Number of beats	Features / Classifier	Accuracy rate
Acharya et al. [8]	• 12 lead • Normal and MI of 10 types.	Normal:125,652 MI: 485,753	• Wavelet transform and 12 non-linear features. • KNN classifier	98.74%
Kumar et al. [9]	• Lead-II • Normal and MI.	Normal: 10,546 MI: 40,182	• FAWT, Sample Entropy • LS-SVM	99.31%
Sharma et al. [10]	• Lead-II, III and aVF • Normal and IMI	HC: 3037 IMI: 3240	• Wavelet transform, sample entropy, sub-band energy, log energy entropy and median slope • SVM	98.84%
Lodhi et al. [24]	• 12 lead • Normal and MI	Normal: 31,722 MI: 49,930	• End-to-end • Convolutional Neural Network	93.53%
Sadhukhan et al. [18]	• Lead II, III and V2 • Normal vs MI	Normal: 5000 MI: 15,000	• Phase of discrete Fourier transform • Logistic regression	95.60%
Dohare et al. [14]	• 12 lead • Normal and MI	549 records from 290 subjects	• Interval features and PCA • SVM	98.96%
Lui et al. [25]	• Lead-I • Normal, MI, other CVD and noisy data	PTB and AF-Challenge database.	• End-to-end • CNN-LSTM	94.62%
Proposed	• 12 lead • Normal and MI of 10 types.	Normal:125,652 MI:485,752	• End-to-end • Convolutional Neural Network	99.78%

2 ECG signal for the classification of normal and MI signals. Sharma et al. [10] achieved 98.84% success using lead II, III and aVF signals to differentiate inferior MI from healthy controls. Lodhi et al. [24] designed a 20-layer CNN model for this problem. The model outputs obtained from 12-lead signal inputs were used for the final estimation with the vote estimator and achieved a performance of 93.53%. Lui et al. [25], using a CNN and recurrent neural network-based approach for multi-class diagnosis of MI as well as other cardiovascular diseases.

From in Table 6, it can be seen that the problem of classification of MI can generally be posed as binary classification problem, i.e. distinguishing normal and MI ECG signals. Acharya et al. [8], have evaluated ten different MI types using handcrafted feature extraction and shallow classifier. They used wavelet transform based 12 non-linear features and KNN classifier. Also, their proposed system obtained low accuracy for some leads i.e., III (86.93%) and aVF (87.93%). The proposed approach in this study is a completely end-to-end structure and is based on deep learning. In addition,

the performance values obtained in this study are better than other studies. The most important advantage of the study is that the proposed CNN method for 12-lead ECG signals can successfully distinguish between 10 different MI types and normal ECG signals with more than 99% classification performance. One limitation of the study is the time cost of the training phase due to the large size of the data. For this reason, high-level equipment such as GPU is needed during the training phase. This difficulty is a situation encountered in almost all deep learning-based studies. However, once trained, there is no time cost during the implementation of the trained models.

5. Conclusion

In this study, we propose a deep CNN model that provides automatic recognition of MI on 12-lead ECG signals. With the proposed CNN model, it is ensured that the signals are classified by an end-to-end structure without any handcrafted feature extraction. In the study, 12-lead signals of 10 different MI types were obtained from PTB diagnostic ECG database. From our results, the lead with the highest classification performance was lead V4 (accuracy 99.78%). Importantly, the proposed CNN model yielded accuracy and sensitivity performance over 99.00% on all lead signals. With this performance, we envisage that this model that can be applied for automated MI detection, including on wearable technologies.

This study provides an effective framework for the automated detection of MI on ECG. Specifically, it is able to detect 10 different MI types with an accuracy of more than 99% and hence can be employed in clinical settings. In future studies, the performance evaluations of the proposed model will be done on the different MI datasets. Moreover, we intend to use the ECG signals of various leads to come out with a three dimensional plot to decipher the location of the heart which is affected by MI.

References

[1] H. Fujita, V.K. Sudarshan, et al., Characterization of cardiovascular diseases using wavelet packet decomposition and nonlinear measures of electrocardiogram signal, in: International Conference on Industrial, Engineering and Other Applications of Applied Intelligent Systems, Springer, 2017, pp. 259–266.

[2] T.V. Kenttä, B.D. Nearing, et al., Prediction of sudden cardiac death with automated high-throughput analysis of heterogeneity in standard resting 12-lead electrocardiograms, Heart Rhythm 13 (3) (2016) 713–720.

[3] U.R. Acharya, H. Fujita, et al., Automated characterization of coronary artery disease, myocardial infarction, and congestive heart failure using contourlet and shearlet transforms of electrocardiogram signal, Knowledge-Based Syst. 132 (2017) 156–166.

[4] R.K. Tripathy, S Dandapat, Detection of cardiac abnormalities from multilead ECG using multiscale phase alternation features, J. Med. Syst. 40 (6) (2016) 143.

[5] M. Sharma, R. San Tan, U.R. Acharya, A novel automated diagnostic system for classification of myocardial infarction ECG signals using an optimal biorthogonal filter bank, Comput. Biol. Med. 102 (2018) 341–356.

[6] H.L. Lu, K. Ong, P Chia, An automated ECG classification system based on a neuro-fuzzy system, in: Computers in Cardiology 2000, IEEE, 2000, pp. 387–390.

[7] L. Sun, Y. Lu, K. Yang, S Li, ECG analysis using multiple instance learning for myocardial infarction detection, IEEE Trans. Biomed. Eng. 59 (12) (2012) 3348–3356.

[8] U.R. Acharya, H. Fujita, et al., Automated detection and localization of myocardial infarction using electrocardiogram: a comparative study of different leads, Knowledge-Based Syst. 99 (2016) 146–156.

[9] M. Kumar, R.B. Pachori, U.R Acharya, Automated diagnosis of myocardial infarction ECG signals using sample entropy in flexible analytic wavelet transform framework, Entropy 19 (9) (2017) 488.

[10] L.D. Sharma, R.K Sunkaria, Inferior myocardial infarction detection using stationary wavelet transform and machine learning approach. Signal, Image Video Process. 12 (2) (2018) 199–206.

[11] S.L. Oh, Y. Hagiwara, et al., Shockable versus nonshockable life-threatening ventricular arrhythmias using DWT and nonlinear features of ECG signals, J. Mech. Med. Biol. 17 (07) (2017) 1740004.

[12] J.T.Y. Weng, J.J. Lin, Y.C. Chen, P.C Chang, Myocardial infarction classification by morphological feature extraction from big 12-lead ECG data, in: Pacific-Asia Conference on Knowledge Discovery and Data Mining, Springer, 2014, pp. 689–699.

[13] P. Kora, S.R Kalva, Improved Bat algorithm for the detection of myocardial infarction, SpringerPlus 4 (1) (2015) 666.

[14] A.K. Dohare, V. Kumar, R Kumar, Detection of myocardial infarction in 12 lead ECG using support vector machine, Appl. Soft Comput. 64 (2018) 138–147.

[15] H. He, Y. Tan, J. Xing, Unsupervised classification of 12-lead ECG signals using wavelet tensor decomposition and two-dimensional Gaussian spectral clustering, Knowledge-Based Syst. 163 (2019) 392–403.

[16] R.K. Tripathy, L.N. Sharma, S Dandapat, A new way of quantifying diagnostic information from multilead electrocardiogram for cardiac disease classification, Healthcare Technol. Lett. 1 (4) (2014) 98–103.

[17] D. Sopic, A. Aminifar, A. Aminifar, D Atienza, Real-time event-driven classification technique for early detection and prevention of myocardial infarction on wearable systems, IEEE Trans. Biomed. Circuits Syst. 12 (99) (2018) 1–11.

[18] D. Sadhukhan, S. Pal, M Mitra, Automated identification of myocardial infarction using harmonic phase distribution pattern of ECG data, IEEE Trans. Instrum. Meas. 67 (99) (2018) 1–11.

[19] S. Padhy, S Dandapat, Third-order tensor based analysis of multilead ECG for classification of myocardial infarction, Biomed. Signal Process. Control 31 (2017) 71–78.

[20] R.J. Martis, C. Chakraborty, A.K Ray, An integrated ECG feature extraction scheme using PCA and wavelet transform, in: India Conference (INDICON), IEEE, 2009, pp. 1–4.

[21] P. Pławiak, Novel methodology of cardiac health recognition based on ECG signals and evolutionary-neural system, Expert Syst. Appl. 92 (2018) 334–349.

[22] M. Barstuğan, R Ceylan, The effect of dictionary learning on weight update of adaboost and ECG classification, J. King Saud Univ.-Comp. Inform. Sci. (2018).

[23] R. Tao, S. Zhang, et al., Magnetocardiography based ischemic heart disease detection and localization using machine learning methods, IEEE Trans. Biomed. Eng. (2018).

[24] A.M. Lodhi, A.N. Qureshi, U. Sharif, Z Ashiq, A novel approach using voting from ecg leads to detect myocardial infarction, in: Proceedings of SAI Intelligent Systems Conference, Springer, 2018, pp. 337–352.

[25] H.W. Lui, K.L Chow, Multiclass classification of myocardial infarction with convolutional and recurrent neural networks for portable ECG devices, Informat. Med. Unlock. 13 (2018) 26–33.

[26] U.R. Acharya, H. Fujita, S.L. Oh, Y. Hagiwara, J.H. Tan, M Adam, Application of deep convolutional neural network for automated detection of myocardial infarction using ECG signals, Inform. Sci. 415 (2017) 190–198.

[27] O. Faust, Y. Hagiwara, T.J. Hong, O.S. Lih, U.R Acharya, Deep learning for healthcare applications based on physiological signals: a review, Comput. Methods Programs Biomed. 161 (2018) 1–13.

[28] Ö. Yıldırım, P. Pławiak, R.S. Tan, U.R. Acharya, Arrhythmia detection using deep convolutional neural network with long duration ECG signals, Comput. Biol. Med. 102 (2018) 411–420 2018.

[29] H. Assodiky, I. Syarif, T Badriyah, Arrhythmia classification using long short-term memory with adaptive learning rate, EMITTER Int. J. Eng. Technol. 6 (1) (2018) 75–91.

[30] S.L. Oh, E.Y. Ng, R. San Tan, U.R Acharya, Automated diagnosis of arrhythmia using combination of CNN and LSTM techniques with variable length heart beats, Comput. Biol. Med. 102 (2018) 278–287.

[31] A.L. Goldberger, L.A. Amaral, et al., PhysioBank, PhysioToolkit, and PhysioNet: components of a new research resource for complex physiologic signals, Circulation 101 (23) (2000) e215–e220.

[32] Chollet, F. Keras: dDeep learning library for theano and tensorflow. URL: https://keras. io, 7(8), 2015.

[33] W. Zhu, N. Zeng, N. Wang, Sensitivity, specificity, accuracy, associated confidence interval and ROC analysis with practical SAS implementations, in: NESUG proceedings: health care and life sciences, 19, Baltimore, Maryland, 2010, p. 67.

[34] Ö. Yıldırım, U.B. Baloglu, U.R Acharya, A deep convolutional neural network model for automated identification of abnormal EEG signals, Neur. Comp. Appl. (2018) 1–12.

[35] P. Pławiak, Novel genetic ensembles of classifiers applied to myocardium dysfunction recognition based on ECG signals, Swarm Evolution. Comp. 39 (2018) 192–208.

[36] P. Pławiak, U.R. Acharya, Novel deep genetic ensemble of classifiers for arrhythmia detection using ECG signals, Neur. Comp. Appl. (2019), doi:10.1007/s00521-018-03980-2.

[37] E.S. Jayachandran, Analysis of myocardial infarction using discrete wavelet transform, J. Med. Syst. 34 (6) (2010) 985–992.